TECHNISCHE MECHANIK, Band 24, Heft 4, (2001), 273-282
Manuskripteingang: 26. Oktober 2001

Modelling of the Creep-damage under the Reversed Stress States by Considering Damage Activation and Deactivation

H. Altenbach, C.-X. Huang, K. Naumenko

Based on the experimental results of copper at 250°C by Murakami and Sanomura (1985), the isotropic and anisotropic damage models as well as the mechanism of the damage activation or deactivation are established and coupled in one constitutive equation. With the help of the finite element method the creep-damage behavior of copper under different stress states is simulated.
The stress state under combined tension and torsion is discussed in detail. In the cases of the spontaneous reversal of the shear stress the rotation of the principal directions of the stress tensor leads to a delayed rotation of the principal strain directions, therefore, a change of the damage state (close or reopen of the micro-cracks) is induced. This phenomenon is modelled by the anisotropic damage model considering the mechanism of the damage activation and deactivation. The predictions are compared with those based on the isotropic model as well as the anisotropic model without the activation mechanism.

1 Introduction

Engineering structures operating at elevated temperatures (higher than 0.3-0.4 times the melting temperature) show a typical creep behavior accompanied by time-dependent creep deformations and damage processes induced by the nucleation and the growth of microscopic cracks and cavities. The evolution of such material damage influences the mechanical state of material. On the last stage before the creep rupture the rapid changes in the stress and the strain state are the consequences observed in many experiments, Riedel (1987).

The main problem arising by creep damage simulation is the formulation of a suitable material model which is able to describe the sensitivity of creep deformation and damage rates to the stress level, the stress state, etc. Such a model has to extrapolate correctly the creep data usually available from uniaxial short-term creep tests (under constant stresses) and realized for narrow stress ranges to the in-service conditions (varying stresses). In addition, the change of the damage state induced by the loading changes has to be considered.

A lot of experimental observations (e.g. Betten et al., 1995; Murakami and Sanomura, 1985) show various disagreements between the experimental results and the numerical simulations based on the isotropic damage concept. In fact the stress state and the evolution of damage affect each other. The orientation of the principal direction of the applied stress tensor (or the applied strain tensor) determines, on one hand, the initial orientations of the cavities and micro-cracks nucleated on grain boundaries and settles the tendency of the anisotropic damage evolution of the materials. Besides, the opened micro-cracks may close as well as the closed micro-cracks may reopen if the stress state changes, Qi and Bertram (1997). On the other hand, the anisotropic properties of the material deterioration result in the redistribution of the stresses different from the isotropic behavior . Since the nature of damage is generally anisotropic the isotropic phenomenon of the material damage may be treated as the special state of the damage anisotropy. Conversely, the isotropic damage models can be extended to models considering the damage induced anisotropy (e.g. Betten, 1983; Cordebois and Sidoroff, 1983; Benallal, 2000; Murakami and Ohno, 2000; Murakami and Ohno, 1981).

Murakami and Sanomura (1985) tested copper at 250°C under varying loading and formulated a model based on a second rank damage tensor in order to describe the creep responses. Although the anisotropic damage model provides better predictions compared with the isotropic one, significant deviations were observed in the case of reversed torsion. As a possibility of the modification the contribution of the creep rates to the damage growth was discussed.

In this paper we put our attention to another possibility for proceeding modification by introducing the mechanism of the damage activation and deactivation in the constitutive model, so that the fact of the state change of the micro-cracks induced by the loading changes can be described, i.e., the damage still exists but the loading condition can render it inactive. For the representation of this mechanism Hansen and Schreyer (1995) proposed

a phenomenological model. Based on this approach, it is possible to couple the damage model and the mechanism of the damage activation and deactivation into the constitutive equation for the creep-damage behavior under varying loads. In our study we implement these coupled models into a finite element code in order to solve the initial-boundary value problem. By modelling the creep tests of the copper at 250°C under combined tension and torsion we can compare the validity of different creep-damage models.

2 Creep-damage Models

If we employ the conventional creep laws of McVetty type, Finnie and Heller (1959), together with the power law damage equation (Kachanov, 1958; Rabotnov, 1969) the constitutive model for isotropic creep behavior can be formulated as

$$\begin{aligned}
&\dot{\varepsilon}^{cr} = \frac{3}{2}\left[A_1\sigma_{vM}^{n_1-1} r\exp(-rt^*)\boldsymbol{s} + A_2\left(\frac{\sigma_{vM}}{1-\omega}\right)^{n_2}\frac{1}{\sigma_{vM}}\boldsymbol{s}\right] \\
&\dot{\omega} = \frac{B(\langle\sigma_{eq}\rangle)^l}{(1-\omega)^k} \qquad 0 \le \omega \le \omega_* \\
&\sigma_{eq} = \alpha\sigma_I + (1-\alpha)\sigma_{vM} \qquad \sigma_{vM} = [3I_2(\boldsymbol{s})]^{\frac{1}{2}} = \left(\frac{3}{2}\boldsymbol{s}\cdot\cdot\boldsymbol{s}\right)^{\frac{1}{2}} \\
&\langle\sigma_{eq}\rangle = \sigma_{eq} \quad \text{for} \quad \sigma_{eq} > 0 \qquad \langle\sigma_{eq}\rangle = 0 \quad \text{for} \quad \sigma_{eq} \le 0
\end{aligned} \tag{1}$$

where the first term in equation (1-1) represents the primary creep and the second term is for secondary and tertiary creep of the Norton-Kachanov type. σ_{vM} is the von Mises equivalent stress, $\boldsymbol{s}$ is the stress deviator. Equation (1-2) represents the evolution of the isotropic damage parameter ω. σ_{eq} is used in the form proposed by Leckie and Hayhurst (1977) with the maximum principal stress σ_I, $I_2(\boldsymbol{s})$ is the second invariant of the stress deviator. t^* is a fictitious time that should be eliminated for problems of variable stresses, Murakami and Sanomura (1985). A_1, n_1, r, A_2, n_2, B, k and l are material constants. Note, the dimensions of A_1 and A_2 depend on the values of the exponents n_1 and n_2. In equation (1-3) α can be used as an influence or weighting factor. The creep equation fulfills the incompressibility condition.

The effective stress based on the isotropic damage concept by Rabotnov (1969) has the form

$$\tilde{\boldsymbol{\sigma}} = \frac{1}{1-\omega}\boldsymbol{\sigma} \tag{2}$$

By applying the effective stress $\tilde{\boldsymbol{\sigma}}$ the damage evolution equation (1-2) can be transformed into its equivalent form

$$\begin{aligned}
&\dot{\omega} = \frac{B(\langle\sigma_{eq}\rangle)^l}{(1-\omega)^k} = B\langle\tilde{\sigma}_{eq}\rangle^k\langle\sigma_{eq}\rangle^{l-k} \\
&\tilde{\sigma}_{eq} = \alpha\tilde{\sigma}_I + (1-\alpha)\tilde{\sigma}_{vM} \qquad \tilde{\sigma}_{vM} = [3I_2(\tilde{\boldsymbol{s}})]^{\frac{1}{2}} = \left(\frac{3}{2}\tilde{\boldsymbol{s}}\cdot\cdot\tilde{\boldsymbol{s}}\right)^{\frac{1}{2}} \\
&\langle\tilde{\sigma}_{eq}\rangle = \tilde{\sigma}_{eq} \quad \text{for} \quad \tilde{\sigma}_{eq} > 0 \qquad \langle\tilde{\sigma}_{eq}\rangle = 0 \quad \text{for} \quad \tilde{\sigma}_{eq} \le 0
\end{aligned} \tag{3}$$

where $\tilde{\sigma}_{vM}$, $\tilde{s}$, $\tilde{\sigma}_{eq}$, $\tilde{\sigma}_I$ and $I_2(\tilde{\boldsymbol{s}})$ are the effective von Mises equivalent stress, the effective stress deviator, the effective damage equivalent stress, the effective maximum principal stress and the second effective stress deviator, respectively.

Based on the isotropic damage concept anisotropic damage models are proposed mostly by introducing the concept of the effective stress tensor as well as the tensor of material constants, Altenbach et al. (1995). According to Lemaitre and Chaboche (1990) the effective stress tensor can be formulated as

$$\tilde{\boldsymbol{\sigma}} = \mathbf{M}\cdot\cdot\boldsymbol{\sigma} \tag{4}$$

where $\mathbf{M}$ is a forth rank tensor depending on the current damage state. Cordebois and Sidoroff (1983) proposed the following expression

$$\mathbf{M} = [\boldsymbol{I} - \boldsymbol{\Omega}]^{-\frac{1}{2}} \wedge [\boldsymbol{I} - \boldsymbol{\Omega}]^{-\frac{1}{2}} \tag{5}$$

where $\boldsymbol{I}$ represents a second rank identity tensor, $\boldsymbol{\Omega}$ is a second rank damage tensor. The composition denoted by the wedge $\wedge$ is defined by $\boldsymbol{A} \wedge \boldsymbol{B} = a_{ij} b_{kl} (\boldsymbol{e}_i \otimes \boldsymbol{e}_k \otimes \boldsymbol{e}_j \otimes \boldsymbol{e}_l)$ for an orthonormal basis $\boldsymbol{e}_i$. In the principal coordinate system of the damage tensor, the matrix form of equation (4) is given by

$$\begin{bmatrix} \tilde{\sigma}_{11} & \tilde{\sigma}_{22} & \tilde{\sigma}_{33} & \tilde{\sigma}_{12} & \tilde{\sigma}_{23} & \tilde{\sigma}_{31} \end{bmatrix}^T = [\mathbf{M}] \begin{bmatrix} \sigma_{11} & \sigma_{22} & \sigma_{33} & \sigma_{12} & \sigma_{23} & \sigma_{31} \end{bmatrix}^T \tag{6}$$

with

$$[\mathbf{M}] = \begin{bmatrix} \frac{1}{1-\Omega_1} & 0 & 0 & 0 & 0 & 0 \\ 0 & \frac{1}{1-\Omega_2} & 0 & 0 & 0 & 0 \\ 0 & 0 & \frac{1}{1-\Omega_3} & 0 & 0 & 0 \\ 0 & 0 & 0 & \frac{1}{\sqrt{(1-\Omega_1)(1-\Omega_2)}} & 0 & 0 \\ 0 & 0 & 0 & 0 & \frac{1}{\sqrt{(1-\Omega_2)(1-\Omega_3)}} & 0 \\ 0 & 0 & 0 & 0 & 0 & \frac{1}{\sqrt{(1-\Omega_3)(1-\Omega_1)}} \end{bmatrix} \tag{7}$$

where σ_{ij} and $\tilde{\sigma}_{ij}$ are the components of $\boldsymbol{\sigma}$ and $\tilde{\boldsymbol{\sigma}}$, respectively, and Ω_1, Ω_2 and Ω_3 denote the principal values of the damage tensor $\boldsymbol{\Omega}$. In addition to (4) and (5), Zheng and Betten (1996) and Betten (2001) have discussed several effective stress tensors in more detail.

To express the evolution of anisotropic damage Chaboche (1982) suggested a representation of the damage tensor as follows:

$$\boldsymbol{\Omega} = d\boldsymbol{R} \tag{8}$$

The evolution of the scalar d can be described by using equation (3-1) after substituting the effective stress tensor (4):

$$\dot{d} = B \langle \tilde{\sigma}_{eq} \rangle^k \langle \sigma_{eq} \rangle^{l-k} \tag{9}$$

The evolution equation of the anisotropic damage tensor has the following form

$$\dot{\boldsymbol{\Omega}} = \dot{d}\boldsymbol{R} = B \langle \tilde{\sigma}_{eq} \rangle^k \langle \sigma_{eq} \rangle^{l-k} \boldsymbol{R} \tag{10}$$

The direction tensor $\boldsymbol{R}$ is defined as

$$\boldsymbol{R} = (1 - k_r)\boldsymbol{S}^+ + k_r \boldsymbol{I} \qquad 0 \leq k_r \leq 1 \tag{11}$$

where the second term represents the isotropic evolution. The anisotropic part can be expressed by the tensor $\boldsymbol{S}^+$ that contains the direction of the positive effective stresses

$$\boldsymbol{S} = \boldsymbol{T} \cdot \tilde{\boldsymbol{\sigma}} \cdot \boldsymbol{T}^T \tag{12}$$

where the transformation tensor $\boldsymbol{T}$ contains the eigenvectors $\boldsymbol{n}^{\sigma_i}, i = 1,2,3$ (i.e. $T_{ij} = n_j^{\tilde{\sigma}_i}$, $n_j^{\tilde{\sigma}_i}$ is the j-th component of the i-th eigenvector), so that the effective stress tensor is transformed into the diagonal form. The positive direction may be filtered by means of the McAulcy-brackets and normalized by the maximal principal tensile stress S^+_{max}. After the retransformation into the original coordinate system we have the normalized positive direction of the effective stress as follows

$$\boldsymbol{S}^+ = \boldsymbol{T}^T \cdot \langle \boldsymbol{S} \rangle \cdot \boldsymbol{T} \frac{1}{S^+_{max}} \tag{13}$$

Introducing the effective stress tensor $\tilde{\boldsymbol{\sigma}}$ and the damage tensor $\boldsymbol{\Omega}$ into the second part of the creep constitutive equation (1-1) we obtain

$$\dot{\varepsilon}^{cr} = \frac{3}{2}\left[A_1\sigma_{vM}^{n_1-1} r\exp(-rt^*)\boldsymbol{s} + A_2\tilde{\sigma}_{vM}^{n_2}\frac{1}{\tilde{\sigma}_{vM}}\tilde{\boldsymbol{s}}\right] \tag{14}$$

3 Mechanism of the Damage Activation and Deactivation

The damage may still exist but eventually does not affect the stiffness of the material, i.e., the damage effects may be activated or deactivated according to the stress and strain state. If the micro-cracks are open, the inner surfaces of them are expected to be stress free, the damage is active and the effective stress is higher than the usual stress. If the micro-cracks are closed under compression, the effective stress is equal to the usual stress, and thus, the damage becomes inactive, Qi and Bertram (1997). In the uniaxial case the damage is active, if

- the total strain ε is positive, because the micro-cracks are open,
- the elastic strain ε^{el} is positive, because the damaged material with closed micro-cracks (ε is negative) can not be in tension.

This relationship may be described by an activation function W^a

$$\omega^a = \omega W^a(\varepsilon, \varepsilon^{el}) \qquad W^a(\varepsilon, \varepsilon^{el}) = 1 - [1 - H(\varepsilon)][1 - H(\varepsilon^{el})] \tag{15}$$

where $H(x)$ is the Heaviside function, Hansen and Schreyer (1995). ω is the damage parameter. ω^a is the active damage parameter.

To extend the uniaxial activation function W^a to multi-axial stress states, one can consider the spectral decomposition of the elastic strain tensor $\boldsymbol{\varepsilon}^{el}$ and the total strain tensor $\boldsymbol{\varepsilon}$

$$\boldsymbol{\varepsilon}^{el} = \sum_{I=1}^{3} \varepsilon_I^{el}\boldsymbol{n}^{\varepsilon_I^{el}} \otimes \boldsymbol{n}^{\varepsilon_I^{el}} \qquad \boldsymbol{\varepsilon} = \sum_{I=1}^{3} \varepsilon_I \boldsymbol{n}^{\varepsilon_I} \otimes \boldsymbol{n}^{\varepsilon_I} \tag{16}$$

where ε_I^{el} and ε_I are the I-th eigenvalues, $\boldsymbol{n}^{\varepsilon_I^{el}}$ and $\boldsymbol{n}^{\varepsilon_I}$ are the corresponding I-th eigenvectors of ε_I^{el} and ε_I, respectively. By means of the Heaviside function the crack opening/closing mechanism can be described with the following tensors

$$\boldsymbol{Q}^{el,+} = \sum_{I=1}^{3} H(\varepsilon_I^{el})\boldsymbol{n}^{\varepsilon_I^{el}} \otimes \boldsymbol{n}^{\varepsilon_I^{el}} \qquad \boldsymbol{Q}^{+} = \sum_{I=1}^{3} H(\varepsilon_I)\boldsymbol{n}^{\varepsilon_I} \otimes \boldsymbol{n}^{\varepsilon_I} \tag{17}$$

where $\boldsymbol{Q}^{+}$ and $\boldsymbol{Q}^{el,+}$ are the tensors defining the positive directions of the total strain tensor and of the elastic strain tensor, respectively. The positive spectral projection operators (forth rank tensors) for the elastic and the total strains are defined as

$$\mathbf{P}^{\mathbf{el},+} = \boldsymbol{Q}^{el,+} \wedge \boldsymbol{Q}^{el,+} \qquad \mathbf{P}^{+} = \boldsymbol{Q}^{+} \wedge \boldsymbol{Q}^{+} \tag{18}$$

The positive projection of the elastic and the total strain tensors are then given by

$$\boldsymbol{\varepsilon}^{el,+} = \mathbf{P}^{el,+} \cdot\cdot \boldsymbol{\varepsilon}^{el} \qquad \boldsymbol{\varepsilon}^{+} = \mathbf{P}^{+} \cdot\cdot \boldsymbol{\varepsilon} \tag{19}$$

An active damage tensor is defined as follows

$$\boldsymbol{\Omega}^a = \mathbf{W}^a \cdot\cdot \boldsymbol{\Omega}, \text{ where } \quad \mathbf{W}^a = \mathbf{I} - (1 - k_a)\left[(\mathbf{I} - \mathbf{P}^{+}) \cdot\cdot (\mathbf{I} - \mathbf{P}^{el,+})\right] \tag{20}$$

and $\mathbf{I}$ is the fourth rank unit tensor. If the parameter $k_a = 1$, $\mathbf{W}^a$ is transformed into the unit tensor $\mathbf{I}$, in this case the damage is always active; if $k_a = 0$, the mechanism of the damage activation and deactivation is included.

Replacing the damage tensor $\mathbf{\Omega}$ by the active damage one $\mathbf{\Omega}^a$ in equation (5) the active effective stress tensor has the form

$$\tilde{\boldsymbol{\sigma}} = \mathbf{M} \cdot\cdot \boldsymbol{\sigma}, \text{ where } \quad \mathbf{M} = [\boldsymbol{I} - \mathbf{\Omega}^a]^{-\frac{1}{2}} \wedge [\boldsymbol{I} - \mathbf{\Omega}^a]^{-\frac{1}{2}} \tag{21}$$

similar to (5), however, $\mathbf{M}$ in (5) is different from $\mathbf{M}$ in (21).

By applying the active damage tensor and the active effective stress tensor we have the creep-damage constitutive model which consists of

- the elastic and creep model, equation (14),
- the damage activation and deactivation by Hanson and Schreyer, equation (20),
- the active effective stress tensor, equation (21),
- the damage operator by Cordebois and Sidoroff, equation (6),
- the evolution equation by Kachanov and Rabotnov, equation (10), as well as the direction formulation by Chaboche, equation (11).

4 Theoretical Prediction and Comparison with Experimental Results

The validity of the models may be analyzed by comparing with the experimental results. Therefore, we apply the constitutive equation for elastic and creep behavior coupled with three damage models as follows:

- the isotropic damage model (Kachanov-Rabotnov model with $k_r = 1$ in equation (11)),
- the anisotropic damage model 1 (with $k_r = 0$ in equation (11) and $k_a = 1$ in equation (20)) as well as
- the active anisotropic damage model 2 (with $k_r = 0$ in equation (11) and $k_a = 0$ in equation (20)).

Murakami and Sanomura (1985) identified the material constants for copper at 250°C from creep curves under constant tension stresses as follows: $E = 87900$ MPa, $\nu = 0.333$, $A_1 = 4.61 \cdot 10^{-6}$ MPa$^{-n_1}$, $n_1 = 1.98$, $r = 0.11$ h^{-1} , $A_2 = 1.2 \cdot 10^{-10}$ MPa$^{-n_2}$/h, $n_2 = 3.43$, $B = 5.52 \cdot 10^{-10}$ MPa^{-l}/h, $l = 3.46$ and $k = 3.46$. The weighting factor $\alpha = 0.75$ is suggested by Murakami and Sanomura (1985) for the isotropic damage model, and $\alpha = 0.68$ for the anisotropic damage model. In the case of the uniaxial tensile loads (with $\sigma_x = 69.3, 60.6, 52.0, 40.0$ and 35.0 MPa, respectively) the introduced material models (the model with a scalar damage parameter (1) as well as the model (14) with anisotropic damage (10) with or without activation (20)) provide the same predictions. The simulation results based on these three models agree well with the experimental data, Figure 1.

In order to discuss the validity of different models in multi-axial cases, we performed the modelling of creep behavior under the combined constant tension and reversed torsion. The corresponding experimental results can be found in Murakami and Sanomura (1985). The tests were performed on tubular specimens loaded by tensile stress σ_x and the shear stress τ_{xy}. The corresponding values were specified in such a manner that the value of the damage equivalent stress $\sigma_{eq} = \alpha\sigma_I + (1-\alpha)\sigma_{vM} = \sigma^*$ was constant and equal to 45 MPa. After the time period $t = 480$ h the reversal of the shear stress was realized so that the direction of the first principal stress was rotated on $\Delta\theta$. Three series of tests were performed with $\Delta\theta = 30°, 60°, 80°$. Figures 2, 3 and 4 show the time variations of the creep strain components. The lines with symbols marked by number 1 represent the experimental data. Those marked by numbers 2, 3 and 4 represent the numerical predictions by the isotropic model, the anisotropic model 1 and model 2, respectively. According to the results of the experiments the rupture times for $\Delta\theta = 30°, 60°$ and $80°$ are $t^*_{exp} = 992, 1360$ and 1504 h, respectively. Since the damage growth is dominantly controlled by the first principal stress the damage evolution after the shear stress reversal will take place on the rotated surface elements. This explains the reason for the prolongation of the rupture time with the increase of $\Delta\theta$. This fact has been confirmed by micrographic observations of damaged copper tubes, Trampczyński et al. (1981). Therefore, the isotropic damage concept underestimate the rupture times, see Figures 2 - 4 and Table 1. The predictions of the rupture times $t^*_{ani-1} = 850$, 1176 and 1342 h by anisotropic model 1 for $\Delta\theta = 30°, 60°$ and $80°$, respectively, show similar trends to those of the experiments. The results are better compared to the isotropic model. The anisotropic

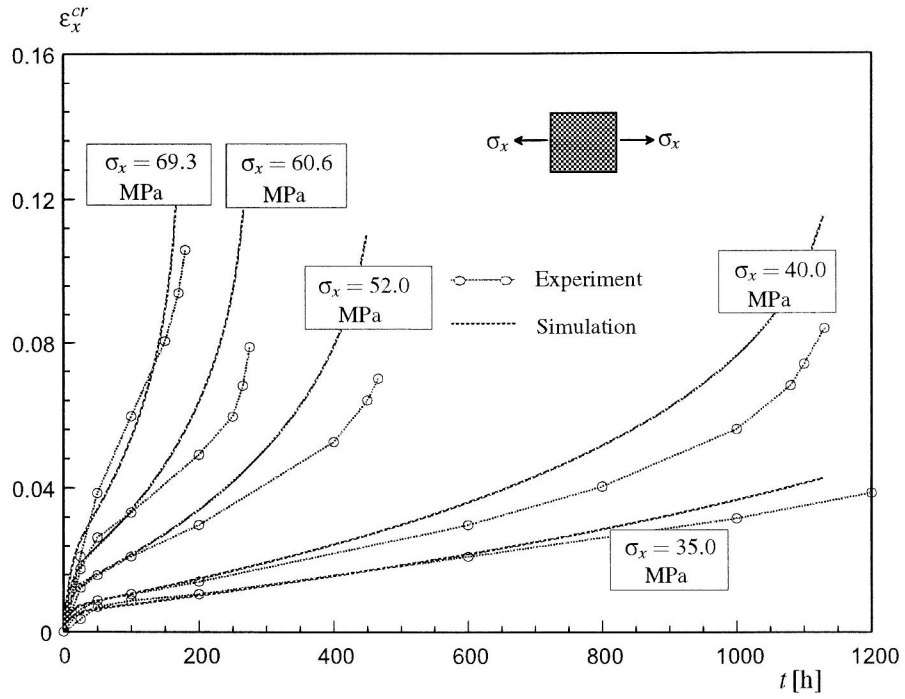

Figure 1. Simulations of Uniaxial Creep Curves of Copper at 250°C, the Experimental Results from Murakami and Sanomura (1985)

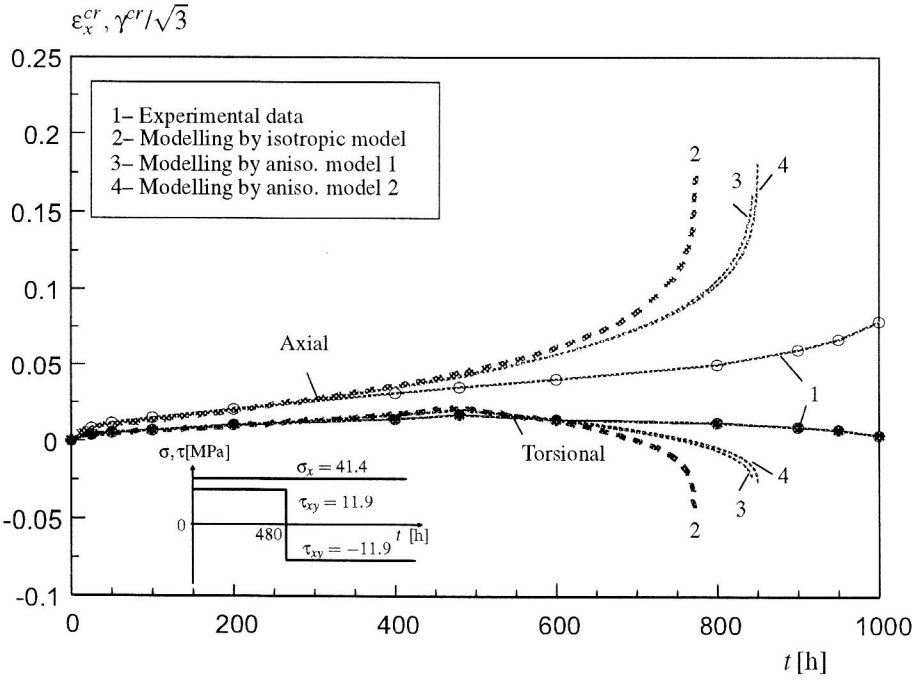

Figure 2. Axial and Torsional Creep Strains under Combined Tension and Reversed Torsion Test ($\sigma^* = 45$MPa, $\Delta\theta = 30°$)

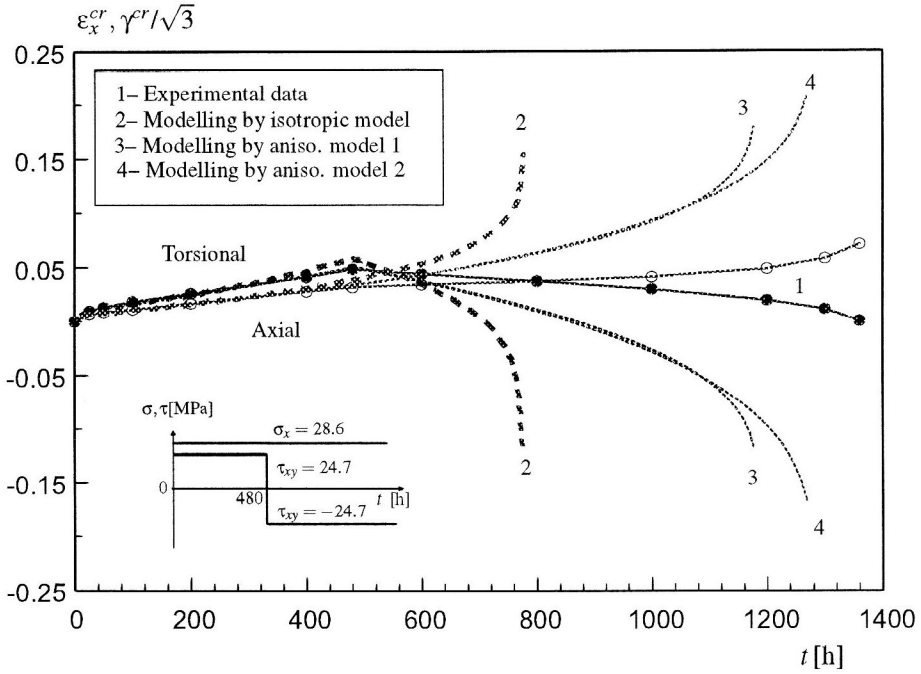

Figure 3. Axial and Torsional Creep Strains under Combined Tension and Reversed Torsion Test ($\sigma^* = 45$MPa, $\Delta\theta = 60°$)

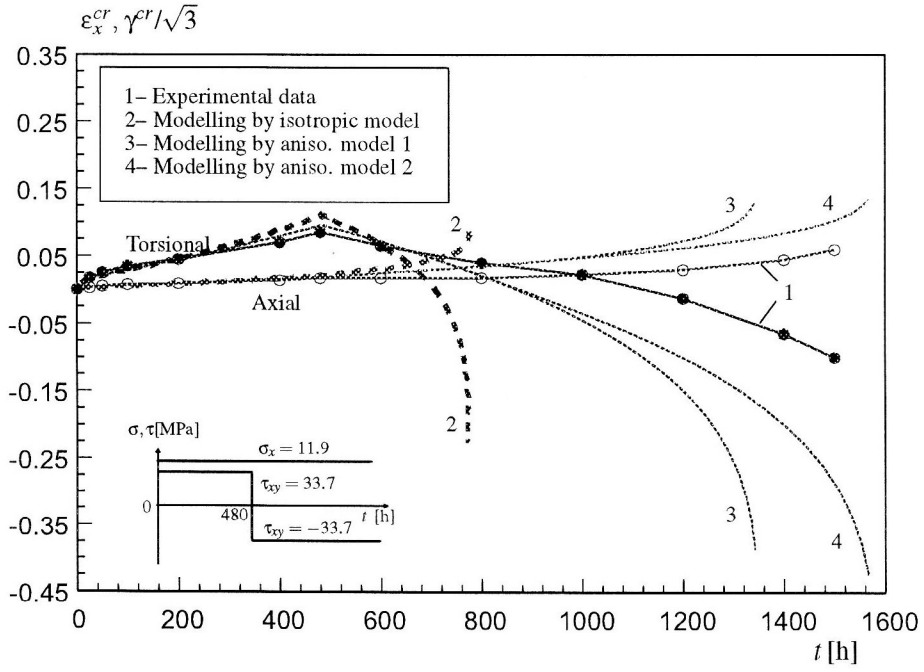

Figure 4. Axial and Torsional Creep Strains Under Combined Tension and Reversed Torsion Test ($\sigma^* = 45$MPa, $\Delta\theta = 80°$)

model 2 predicts the rupture times $t^*_{ani-2} = 854, 1268$ and 1567 h for $\Delta\theta = 30°, 60°$ and $80°$, respectively. These predictions are more accurate compared to the anisotropic model 1, for instance, in the case of $\theta = 80°$ the ratio of the predicted rupture time to the corresponding experimental value is $t^*_{ani-2}/t^*_{exp} = 1.04$.

Finally, we discuss now the creep response of the damaged material. The experiments show that the shear creep rates after stress change at 480 h are reduced always by $30 \sim 50$ percent in comparison with the minimum creep rates before the stress change, Figures 2 - 4. The anisotropic model 1 describes the creep behavior up to the stress change better than the isotropic model, but its prediction of the succeeding creep has to be modified. Compared to the anisotropic model 1, the model 2 leads to better predictions of the creep response. In the case of $\Delta\theta = 80°$, for instance, the predictions of creep strains by the anisotropic model 2 are significantly improved, Figure 4.

	Experiment	Isotropic model	Anisotropic model 1	Anisotropic model 2
Life times	t^*_{exp} [h]	t^*_{iso} [h]	t^*_{ani-1} [h]	t^*_{ani-2} [h]
$\Delta\theta = 30°$	992	771	850	854
$\Delta\theta = 60°$	1360	773	1176	1268
$\Delta\theta = 80°$	1504	773	1342	1567
Proportion	$t*_{exp}/t*_{exp}$	t^*_{iso}/t^*_{exp}	t^*_{ani-1}/t^*_{exp}	t^*_{ani-2}/t^*_{exp}
$\Delta\theta = 30°$	1	0.78	0.85	0.86
$\Delta\theta = 60°$	1	0.57	0.86	0.93
$\Delta\theta = 80°$	1	0.51	0.89	1.04

Table 1. Comparison of the Rupture Times Obtained by Different Models with Experimental Results

In addition, we discuss the evolution of the damage parameter ω according to the isotropic model and the damage components Ω_{ij} as well as Ω^a_{ij} according to the anisotropic models 1 and 2, respectively. The equivalent stress $\tilde{\sigma}_{eq}$ which controlls the damage evolution is not the same in the isotropic and anisotropic models. In the last case $\tilde{\sigma}_{eq}$ becomes additionally direction dependent. As a result the rate of the damage components Ω_{ij} by the anisotropic models is generally smaller than that of the damage parameter ω in the isotropic model, see Figure 5(a), and a longer life time is predicted by the anisotropic model 1. Figure 5(b) shows the time variations of the damage components Ω_{ij} and of the activated damage components Ω^a_{ij} by the anisotropic model 2. Compared to the anisotropic model 1 the rates of the damage components Ω_{ij} are further reduced and lead to longer life time. The crosses of the curves for Ω_{ij} and for Ω^a_{ij} result from the damage deactivation caused by the delayed rotation of the principal strains and the redistribution of the strain components after the stress change at 480 h.

5 Conclusions

The purpose of this paper was the numerical study of creep behavior of copper under complex stress states by using different damage models. By comparing with experimental results the following conclusion can be given:

- Three concepts for description of the creep-damage process (the isotropic concept as well as two anisotropic concepts with or without the activation mechanism) can be conveniently included in one constitutive model. In the case of the multi-axial stress states the anisotropic models lead to much better predictions than the isotropic model.
- The rotation of the principal stress induced by the reversed loading leads to the redistribution of the strains and induces the state change of the micro-cracks. To describe this phenomenon the active damage tensor and active effective stress tensor are applied. The numerical modelling shows an improvement of predicted rupture times and creep curves.
- Further modification of the anisotropic model with the mechanism of the damage activation and deactivation is still necessary, because the hardening phenomenon must be taken into account especially for the varying loads.

Acknowledgement

The authors gratefully acknowledge the financial support from German Research Foundations (DFG) under grant AL 341/15-1, 2

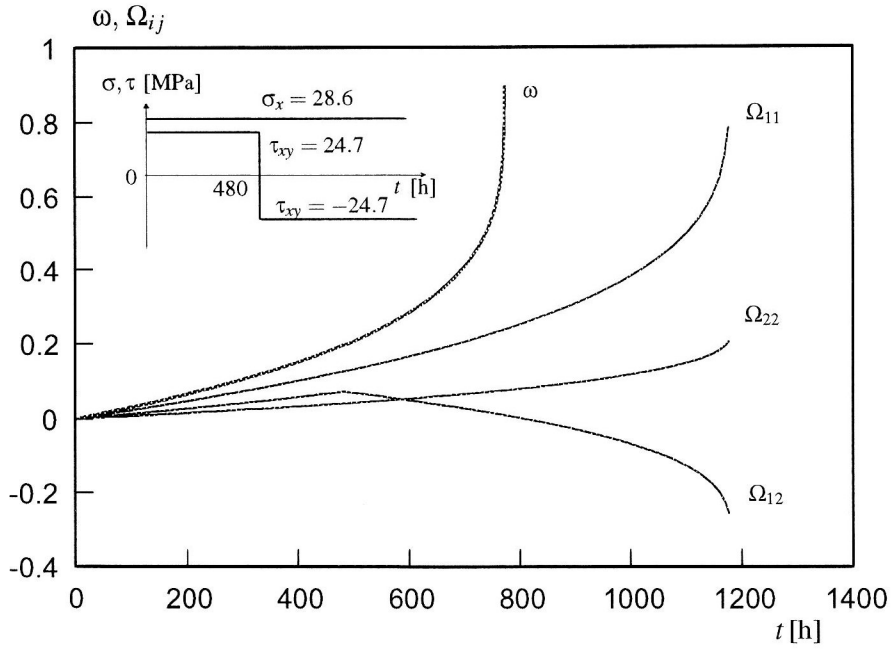

(a)

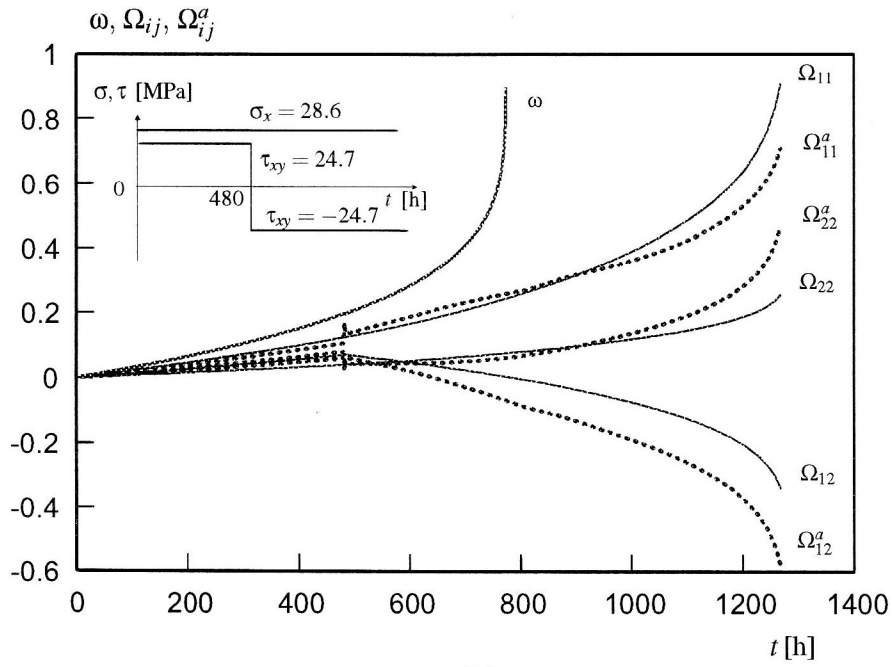

(b)

Figure 5. Time Variations of the Damage Parameter ω, as well as of the Components Ω_{ij} and Ω^a_{ij} of the Damage Tensor ($\sigma^* = 45$MPa, $\Delta\theta = 60°$): (a) ω according to the Isotropic Model and Ω_{ij} according to the Anisotropic Model 1, (b) ω according to the Isotropic Model and $\Omega_{ij}, \Omega^a_{ij}$ according to the Anisotropic Model 2

Literature

1. Altenbach, H.; Altenbach, J.; Zolochevsky, A.: Erweiterte Deformationsmodelle und Versagenskriterien der Werkstoffmechanik. Stuttgart: Deutscher Verlag für Grundstoffindustrie (1995).
2. Benallal, A., editor: Continuous Damage and Fracture. Paris: Elsevier (2000).
3. Betten, J.: Damage Tensors in Continuum Mechanics. Journal de Mécanique théorique et appliquée, 2, 1, (1983), 13–32.
4. Betten, J.; El-Magd, E.; Meydanli, S.; Palmen, P.: Bestimmung der Materialkennwerte einer drei–dimensionalen Theorie zur Beschreibung des tertiären Kriechverhaltens austenitischer Stähle auf der Basis der Experimente. Arch. Appl. Mech., 65, (1995), 110–120.
5. Betten, J.: Mathematical Modelling of Materials Behavior under Creep Conditions. Applied Mechanics Review, 54, (2001), 107-132.
6. Chaboche, J.-L.: Le Concept de Contrainte Effective Appliqué à l'Elasticité et à la Viscoplasticité en Présence d'un Endommagement Anisotrope, In:. Proceedings of the Euromech Colloquium, 115, (1982), 737–760.
7. Cordebois, J.; Sidoroff, F.: Damage Induced Elastic Anisotropy. In: Mechanical Behaviours of Anisotropic Solids (edited by J.P. Boehler). pages 761–774, Boston: Martinus Nijhoff Publishers (1983).
8. Finnie, I.; Heller, W.: Creep of Engineering Materials. New York: McGraw-Hill (1959).
9. Hansen, N. H.; Schreyer, H. L.: Damage Deactivation. Trans. ASME. J. Appl. Mech., 62, (1995), 450–458.
10. Kachanov, L.: On Rupture Time under Condition of Creep. Izv. Akad. Nauk SSSR. Otd. Tekhn. Nauk, 8, (1958), 26–31 (in Russian).
11. Leckie, F.; Hayhurst, D.: Constitutive Equations for Creep Rupture. Acta Metall., 25, (1977), 1059–1070.
12. Lemaitre, J.; Chaboche, J.-L.: Mechanics of Solid Materials. Cambridge University Press (1990).
13. Murakami, S.; Ohno, N.: A Continuum Theory of Creep and Creep Damage. In: Creep in Structures (edited by A.R.S. Ponter and D.R. Hayhurst). pages 422–444, Springer, Berlin (1981).
14. Murakami, S.; Ohno, N., editors: IUTAM Symposium on Creep in Structures. Dordrecht: Kluwer Academic Publishers (2000).
15. Murakami, S.; Sanomura, Y.: Creep and Creep Damage of Copper under Multiaxial States of Stress. In: Plasticity Today (edited by A. Sawczuk and G. Bianci). pages 535–551, London: Elsevier Appl. Sci. (1985).
16. Qi, W.; Bertram, A.: Anisotropic Creep Damage Modeling of Single Crystal Superalloys. Technische Mechanik, 17, 4, (1997), 313–322.
17. Rabotnov, Y.: Creep Problems in Structural Members. Amsterdam: North Holland (1969).
18. Riedel, H.: Fracture at High Temperatures. Berlin: Springer (1987).
19. Trampczyński, W.; Hayhurst, D.; Leckie, F.: Creep Rupture of Copper and Aluminium under Non-proportional Loading. J. Mech. Phys. Solids, 29, (1981), 353–374.
20. Zheng Q.-S.; Betten, J.: On Damage Effective Stress and Equivalence Hypothesis. Int. J. of Damage Mechanics, 5, (1996),219–240.

Address: Prof. Dr.-Ing. Holm Altenbach, Dr.-Ing. Chunxiao Huang, Dr.-Ing. Konstantin Naumenko, Fachbereich Ingenieurwissenschaften, Lehrstuhl für Technische Mechanik, Martin-Luther-Universität Halle-Wittenberg, D-06099 Halle.

e-mail: holm.altenbach@iw.uni-halle.de